

We are IntechOpen, the world's leading publisher of Open Access books Built by scientists, for scientists

4,800

Open access books available

122,000

International authors and editors

135M

Downloads

Our authors are among the

154

Countries delivered to

TOP 1%

most cited scientists

12.2%

Contributors from top 500 universities



WEB OF SCIENCE™

Selection of our books indexed in the Book Citation Index
in Web of Science™ Core Collection (BKCI)

Interested in publishing with us?
Contact book.department@intechopen.com

Numbers displayed above are based on latest data collected.
For more information visit www.intechopen.com



Superallocation and Cluster-Based Cooperative Spectrum Sensing in 5G Cognitive Radio Network

Md Sipon Miah, Md Mahbubur Rahman and Heejung Yu

Additional information is available at the end of the chapter

<http://dx.doi.org/10.5772/66047>

Abstract

Consequently, the research and development for the 5G systems have already been started. This chapter presents an overview of potential system network architecture and highlights a superallocation technique that could be employed in the 5G cognitive radio network (CRN). A superallocation scheme is proposed to enhance the sensing detection performance by rescheduling the sensing and reporting time slots in the 5G cognitive radio network with a cluster-based cooperative spectrum sensing (CCSS). In the 4G CCSS scheme, first, all secondary users (SUs) detect the primary user (PU) signal during a rigid sensing time slot to check the availability of the spectrum band. Second, during the SU reporting time slot, the sensing results from the SUs are reported to the corresponding cluster heads (CHs). Finally, during CH reporting time slots, the CHs forward their hard decision to a fusion center (FC) through the common control channels for the global decision. However, the reporting time slots for the SUs and CHs do not contribute to the detection performance. In this chapter, a superallocation scheme that merges the reporting time slots of SUs and CHs by rescheduling the reporting time slots as a nonfixed sensing time slot for SUs to detect the PU signal promptly and more accurately is proposed. In this regard, SUs in each cluster can obtain a nonfixed sensing time slot depending on their reporting time slot order. The effectiveness of the proposed chapter that can achieve better detection performance under -28 to -10 dB environments and thus reduce reporting overhead is shown through simulations.

Keywords: 5G, software-defined network, cognitive radio, superallocation technique, cluster head, fusion center

1. Introduction

Around 2020, the promising 5G technology in cognitive radio networks is expected to be developed 5G networks that will have to support advanced services and multimedia

applications with a wide variety of requirements, including higher peak and user data rates, reduced latency, enhanced indoor and outdoor coverage, improved energy efficiency, capacity and throughput, network densification, autonomous applications and network management, and Internet of things [1, 2].

The primary technologies and approaches to address the requirements for the 5G systems can be classified as follows [1, 2]:

- Network densification of existing mobile cellular networks (e.g., peer-to-peer [P2P], machine-to-machine [M2M], device-to-device [D2D], and heterogeneous networks);
- Full-duplex (FD) communication (e.g., simultaneous transmission and reception);
- Improvement of capacity and throughput (e.g., massive multiple-input multiple-output [massive MIMO]);
- Improvement of energy efficiency by wireless charging and energy harvesting;
- Advanced services and applications by a cloud-based radio access network (C-RAN) (e.g., smart city and service-oriented communication);
- Multiple network operators to share common resources by cooperation and network virtualization (e.g., network infrastructure, backhaul, licensed spectrum, core and radio access network, energy/power, etc.).

In this chapter, the main objectives of the beyond 2020 5G cognitive radio network by providing the technical support that needed to address the very challenging requirements foreseen for this time frame are proposed. A 5G system (i) has to be significantly more efficient in terms of energy, cost, and resource utilization (e.g., licensed spectrum utilization) than today's system (e.g., 4G); (ii) has to be significantly more versatile to support a significant diversity of requirements; and (iii) should provide better scalability in terms of the number of connected devices, densely deployed access points, spectrum usage, energy, and cost. In CRN, both higher data volume and higher data rates are required to access more spectrum band. As mentioned before, in 4G, it is clearly expected that more spectrum will be released for licensed wireless mobile communications. This new spectrum lies in the frequency range between 300 MHz and 6 GHz. However, for the future 5G system, these new spectrum opportunities will not be sufficient. Moreover, wireless local area networks operating in the unlicensed bands, such as the ISM and U-NII bands at 2.4 and 5 GHz, as well as the 60 GHz band, can be more tightly integrated. The present chapter discusses the superallocation and cluster-based cooperative spectrum sensing in the 5G CRN (e.g., highlights the number (i)) to provide more efficient spectrum utilization.

Cognitive radio (CR) is a new promising technology in the wireless communication era that has changed the policy of spectrum allocation from a static to a more flexible paradigm [3]. Recently, CRs that enable opportunistic access to underutilized licensed bands have been proposed as a promising technology for the improvement of spectrum operations. In an overlay cognitive radio network, an overlay waveform is used to exploit idle spectra and

transmit information data within these unused regions. On the other hand, in an underlay cognitive radio network an underlay waveform with low transmit power is used to transmit data without harmful effects on the primary network [4]. In this chapter, we focus on overlay networks where secondary users find the idle channel with spectrum sensing. A precondition of secondary access is that there shall be no interference with the primary system [5]. This means spectrum sensing plays a vital role in the 5G CRN.

There are a number of spectrum sensing techniques, including matched filter detection, cyclostationary detection, and energy detection [6–8]. Matched filter detection is known as the optimum method for detection of the primary users when the transmitted signal is known. The main advantage of matched filtering is that it takes a short time to achieve spectrum sensing below a certain value for the probability of false alarm or the probability of detection compared to the other methods. However, it requires complete knowledge of the primary user's signaling features, such as bandwidth, operating frequency, modulation type and order, pulse shaping, and packet format. Cyclostationary detection is especially appealing because it is capable of differentiating the primary signal from the interference and noise. Due to noise rejection property, it works even in a very low signal-to-noise ratio (SNR) region, where the traditional signal detection method such as the energy detection is used. It offers good performance but requires knowledge of the PU cyclic frequencies and also requires a long time to complete sensing. On the other hand, the energy detection senses spectrum holes by determining whether the primary signal is absent or present in a given frequency slot. It operates without the knowledge of the primary signal parameters. Its key parameters, including detection threshold, number of samples, and estimated noise power, determine the detection performance. Also, it is an attractive and suitable method due to its easy implementation and low computation complexity. However, it is vulnerable to the uncertainty of noise power and cannot distinguish between noise and signal. Conversely, its major limitation is that the received signal strength can be dangerously weakened at a particular geographic location due to multipath fading and the shadow effect [9].

In order to improve the reliability of spectrum sensing, cooperative spectrum sensing was proposed [10–13]. Each SU performs local spectrum sensing independently and then forward the sensing results to the fusion center (FC) through the noise-free reporting channels between the SUs and the FC. In Zarrin and Lim [13], basic methods including AND, OR, and k-out-of-N logic are used to take hard decisions for a final decision at the FC. However, the reporting channels are always subject to fading effects in real environments [14]. When reporting channels become very noisy, cooperative sensing offers no advantages [15–16]. To overcome this problem, Sun et al. [17] and Xia et al. [18] proposed a cluster-based cooperative sensing scheme by dividing all the SUs into a number of clusters and selecting the most favorable SU in each cluster as a CH to report the sensing results, which can dramatically reduce the performance deterioration caused by fading of the wireless channels. In these schemes, the SU selected as the CH has to fuse sensing data from all cluster members (the SUs in this cluster). However, in these schemes, each SU's reporting time slot and the CH reporting time slot offer no contribution to spectrum sensing, while SU sensing and reporting times and CH reporting time are in different time slots.

Jin et al. [19] proposed a superposition-based cooperative spectrum-sensing scheme that increases the sensing duration by superposing the SUs' reporting duration into the sensing duration. However, this scheme adopts various individual reporting durations. In this case, synchronization problems occur at the FC. Moreover, the data processing burden at the FC increases for a large CR network.

In this chapter, we propose a superallocation and cluster-based cooperative spectrum sensing 5G scheme to provide more efficient spectrum sensing. In this scheme, each SU achieves a nonfixed and longer sensing time for sensing the PU signal bandwidth because both the SUs and the CHs are superallocated to different reporting time slots. On the other hand, both the SU and the CH reporting time slots are of fixed length because the synchronization problem for the FC is relieved. In addition, this proposed scheme decreases the data processing burden of the FC while all the SUs in the CRN are divided into fewer clusters such that each SU reports its local decision to the corresponding CH, which then reports to the FC. Simulation results show that the proposed 5G scheme can improve sensing performance in a low signal-to-noise ratio environment (i.e., -28 dB) and also greatly reduces reporting overhead in comparison with cluster-based cooperative spectrum sensing in 4G CRNs.

The remainder of this chapter is organized as follows. Section 2 describes the system model. Section 3 offers an overview of energy detection. Section 4 describes the cluster-based cooperative spectrum sensing in the 4G CRN. The proposed superallocation and cluster-based cooperative spectrum sensing in the 5G CRN is presented in Section 5 that addresses the spectrum utilization goal of this chapter for the 5G CRN. Some simulations and comparisons are presented in Section 6. We finally present the main conclusion of this chapter in Section 7.

2. Cognitive radio network system model

In CRN, the detection performance of the PU signal might be degraded when the sensing decisions are forwarded to an FC through fading channels. **Figure 1** shows the CRN deployment where SUs are grouped into a cluster governed by a CH based on low-energy adaptive clustering hierarchy-centralized (LEACH-C) protocol [20] and the CHs of the clusters report their decisions to an FC through a common control channel. Here, HDF will be applied to obtain a final decision on the presence of the PU activities. The process of the LEACH-C protocol is made up of several rounds, and each round consists of two phases: a setup phase when the CHs and clusters are organized and a steady-state phase when the cluster members begin to send their measurements to CH and CHs send their decision to the FC. In the setup phase, each SU sends information about its current location and SNR of reporting channel to the FC. Based on this information, the FC determines CHs among all CRUs, while the remaining CRUs will act as cluster members. After the CHs are determined, the FC broadcasts a message that contains not only the CH ID for each SU but also the information of time synchronization. If an SU's CH ID matches its own ID, the SU is a CH; otherwise, the SU is a cluster member and goes to sleep. In the steady-state phase, the SUs start to forward the measurement of the received PU's signal to the CH, and then the CH collects the measurements from the cluster members and makes the cluster decision about the presence of the PU and sends it to the FC during their allocated reporting time slots. Afterward, the FC combines

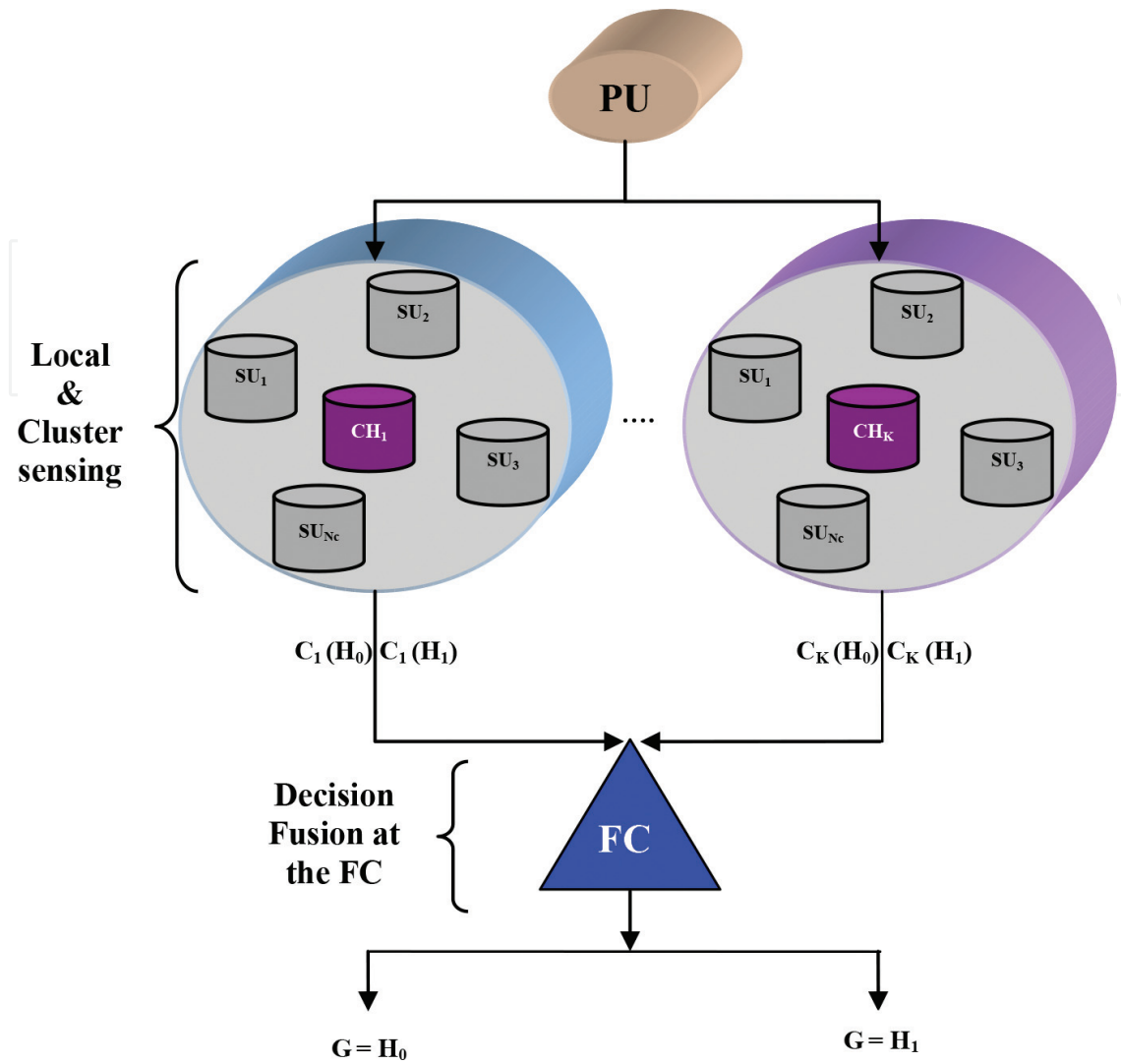


Figure 1. Cluster-based cooperative spectrum sensing in the 5G cognitive radio network.

the received clustering decision to make the final decision, then broadcasts it back to all CHs and the CHs send it to their cluster members.

Spectrum sensing can be formulated as a binary hypothesis-testing problem as follows:

$$\begin{cases} H_1 : \text{PU signal is present,} \\ H_0 : \text{PU signal is absent.} \end{cases} \quad (1)$$

Each SU implements a spectrum sensing process that is called local spectrum sensing to detect the PU's signal. According to the status of the PU, the received signal of an SU can be formulated as follows:

$$y_j(t) = \begin{cases} \eta_j(t), & H_0 \\ h_j(t)x(t) + \eta_j(t), & H_1 \end{cases} \quad (2)$$

where $y_j(t)$ represents the received signal at the j th SU, $h_j(t)$ denotes the gain of the channel between the j th SU and the PU, $x(t)$ with variance of σ_x^2 represents the signal transmitted by the

PU, and $\eta_j(t)$ is a circularly symmetric complex Gaussian (CSCG) with variance of $\sigma_{\eta,j}^2$ at the j th SU.

In addition, we make the following assumptions [21]:

- $x(t)$ is a binary phase shift keying (BPSK) modulated signal.
- $x(t)$ and $\eta_j(t)$ are mutually independent random variables.
- The SU has complete knowledge of noise and signal power.

Cluster-based cooperative spectrum sensing in a 5G CRN is shown in **Figure 1**, which contains N SUs, K clusters, and one FC. In this network, all the SUs are separated into K clusters, in which each cluster contains N_c SUs; and the cluster head CH_k , $k = 1, 2, \dots, K$, is selected to process the collected sensing results from all SUs in the same cluster.

For sensing duration, first, each SU calculates the energy of its received signal in the frequency band of interest. Local decisions are then transmitted to the corresponding CH through a control channel, which will combine local decisions to make a cluster decision. Second, all cluster decisions will be forwarded to the FC through a control channel. At the FC, all cluster decisions from the CHs will be combined to make a global decision about the presence or the absence of the PU signal.

3. Overview of energy detection

The energy detection method has been demonstrated to be simple, quick, and able to detect primary signals, even if prior knowledge of the signal is unknown [22–25]. A block diagram of the energy detection method in the time domain is shown in **Figure 2**. To measure the energy of the signal in the frequency band of interest, a band-pass filter is first applied to the received signal, which is then converted into discrete samples with an analog-to-digital (A/D) converter.

An estimation of the received signal power is given by each SU with the following equation:

$$E_j = \frac{1}{L} \sum_{t=1}^L |y_j(t)|^2 \quad (3)$$

where $y_j(t)$ is the t th sample of a received signal at the j th SU and L is the total number of samples. $L = T_s F_s$, where T_s and F_s are the sensing time and signal bandwidth in hertz, respectively. According to the central limit theorem, for a large number of samples, e.g., $L > 250$, the probability distribution function (PDF) of E_j , which is a chi-square distribution

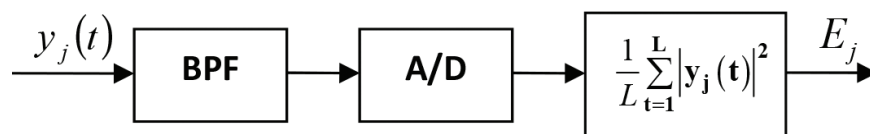


Figure 2. Block diagram of the energy detection scheme.

under both hypothesis H_0 and hypothesis H_1 , can be well approximated as a Gaussian random variable such that

$$E_j = \begin{cases} N(\mu_{0,j}, \sigma_{0,j}^2) \\ N(\mu_{1,j}, \sigma_{1,j}^2) \end{cases} \quad (4)$$

where $N(\mu, \sigma^2)$ denotes a Gaussian distribution with mean of μ and variance of σ^2 , $\mu_{0,j}$ and $\sigma_{0,j}^2$ represent the mean and variance, respectively, for hypothesis H_0 , and $\mu_{1,j}$ and $\sigma_{1,j}^2$ represent the mean and variance for hypothesis H_1 .

Lemma 1. When the primary signal is a BPSK-modulated signal and noise is a CSCG, the decision rule in Eq. (4) is modified as follows:

$$E_j = \begin{cases} N\left(\sigma_\eta^2, \frac{1}{L}\sigma_\eta^4\right) \\ N\left(\sigma_\eta^2(1 + \gamma), \frac{1}{L}(1 + 2\gamma)\sigma_\eta^4\right) \end{cases} \quad (5)$$

where $\gamma = \frac{\sigma_x^2}{\sigma_\eta^2}$ that is the SNR of the primary signal at the j th SU. The SNR is a constant in the nonfading additive white Gaussian noise environment [25]. Here, we omit the subscript of j in $\sigma_{\eta,j}^2$, which denotes that index of SU, to simplify the notation.

Proof. For hypothesis H_1 , the mean $\mu_{1,j}$ is expressed as

$$\begin{aligned} \mu_{1,j} &= \sigma_x^2 + \sigma_\eta^2 = \sigma_\eta^2 \left(1 + \frac{\sigma_x^2}{\sigma_\eta^2}\right) \\ &= (1 + \gamma)\sigma_\eta^2 \end{aligned} \quad (6)$$

From Boyed and Vandenberghe [26], variance $\sigma_{1,j}^2$ is

$$\sigma_{1,j}^2 = \frac{1}{L} [E|x(t)|^4 + E|\eta(t)|^4 - (\sigma_x^2 - \sigma_\eta^2)^2] \quad (7)$$

For a complex M -array quadrature amplitude modulation signal [27], $E|x(t)|^4$ is given as

$$E|x(t)|^4 = \left(3 - \frac{2(4M-1)}{5(M-1)}\right)\sigma_x^4 \quad (8)$$

For the BPSK signal [27], then we set $M = 4$. By substituting the value $M = 4$ into Eq. (8), we obtain

$$E|x(t)|^4 = \sigma_x^4 \quad (9)$$

For the CSCG noise signal [26], $E|\eta(t)|^4$ is given as

$$E|\eta(t)|^4 = 2\sigma_\eta^4 \quad (10)$$

Substituting the values $E|x(t)|^4$ and $E|\eta(t)|^4$ into Eq. (7), we obtain

$$\begin{aligned} \sigma_{1,j}^2 &= \frac{1}{L} [\sigma_x^4 + 2\sigma_\eta^4 - (\sigma_x^4 - 2\sigma_x^2\sigma_\eta^2 + \sigma_\eta^4)] \\ &= \frac{1}{L} [\sigma_\eta^4 + 2\sigma_x^2\sigma_\eta^2] = \frac{1}{L} \left[1 + 2\frac{\sigma_x^2}{\sigma_\eta^2} \right] \sigma_\eta^4 \\ &= \frac{1}{L} [1 + 2\gamma] \sigma_\eta^4. \end{aligned} \quad (11)$$

For hypothesis H_0 , substituting the value $\sigma_x^2 = 0$ into Eq. (6), mean $\mu_{0,j}$ is expressed as

$$\mu_{0,j} = \sigma_\eta^2 \quad (12)$$

Again, substituting the value $\sigma_x^2 = 0$ into Eq. (7), variance $\sigma_{0,j}^2$ is expressed as

$$\begin{aligned} \sigma_{0,j}^2 &= \frac{1}{L} [E|\eta(t)|^4 - (\sigma_\eta^2)^2] \\ &= \frac{1}{L} [2\sigma_\eta^4 - \sigma_\eta^4] \\ &= \frac{1}{L} \sigma_\eta^4 \end{aligned} \quad (13)$$

Then, we can have distributions of a decision statistic under null and alternative hypotheses as in Eq. (5).

By the definition of a false alarm probability in a hypothesis testing with a decision statistic of E_j depending on T_s , and a decision threshold of λ_j , the probability of false alarm for the j th SU is given by

$$\begin{aligned} P_f^j(T_s, \lambda_j) &= \Pr[E_j \geq \lambda_j | H_0] \\ &= Q\left(\frac{\lambda_j - \mu_{0,j}}{\sqrt{\sigma_{0,j}^2}}\right) \end{aligned} \quad (14)$$

where $Q(x)$ is the Gaussian tail function given by $Q(x) = \frac{1}{\sqrt{2\pi}} \int \exp\left(-\frac{t^2}{2}\right) dt$. Form Lemma 1, the probability of false alarm under a CSCG noise is given by

$$P_f^j(T_s, \lambda_j) = Q\left(\left(\frac{\lambda_j}{\sigma_\eta^2} - 1\right) \sqrt{T_s F_s}\right) \quad (15)$$

By the definition of a probability of detection in hypothesis testing and Lemma 1, the detection probability for the BPSK-modulated primary signal under a CSCG noise for the j th SU is given by

$$\begin{aligned}
 P_d^j(T_s, \lambda_j) &= \Pr[E_j \geq \lambda_j | H_1] \\
 &= Q\left(\frac{\lambda_j - \mu_{1,j}}{\sqrt{\sigma_{1,j}^2}}\right) \\
 &= Q\left(\left(\frac{\lambda_j}{\sigma_\eta^2} - \gamma - 1\right) \sqrt{\frac{T_s F_s}{(1 + 2\gamma)}}\right)
 \end{aligned}
 \tag{16}$$

The last equality is obtained by using Eq. (5).

With Eqs. (15) and (16), the probabilities of false alarm and the detection of the PU signal can be calculated when the duration of sensing time T_s is given.

4. Cluster-based cooperative spectrum sensing in the 4G CRN

A general frame structure for the cluster-based cooperative spectrum sensing in the 4G CRN is shown in **Figure 3**. With this frame structure, all local decisions are forwarded to the CHs in the scheduled SU reporting time slots and are then forwarded to the FC in the scheduled CH reporting time slots.

Lemma 2. In the cluster-based cooperative spectrum sensing in the 4G CRN, the N SUs in the network adopted fixed sensing time slot T_s^{con} are given by

$$T_s^{\text{con}} = \frac{1}{F_s \gamma^2} \left[Q^{-1}(P_f^j) - Q^{-1}(P_d^j) \sqrt{(1 + 2\gamma)} \right]^2
 \tag{17}$$

to sense the PU's signal with false alarm and detection probabilities of P_f^j and P_d^j , respectively. Here, the superscript "con" means the conventional or 4G CRN.

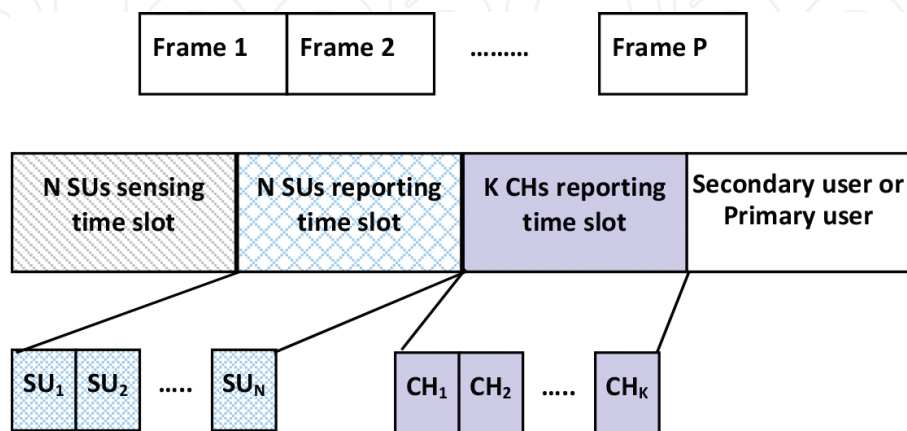


Figure 3. A cluster-based cooperative spectrum sensing in a 4G CRN [18].

Proof: We focus on the BPSK signal and CSCG noise. The probability of detection can be obtained with Eq. (18) by using Eq. (17):

$$\left(\frac{\lambda_j}{\sigma_\eta^2} - \gamma - 1\right) \sqrt{\frac{T_s F_s}{(1 + 2\gamma)}} = Q^{-1}(P_d^j) \quad (18)$$

From Eq. (15), the probability of false alarm can be obtained by

$$\left(\frac{\lambda_j}{\sigma_\eta^2} - 1\right) \sqrt{T_s F_s} = Q^{-1}(P_f^j). \quad (19)$$

By substituting Eq. (19) into Eq. (18) and rewriting this equation, we have

$$\begin{aligned} \left(\frac{Q^{-1}(P_f^j)}{\sqrt{T_s F_s}} - \gamma\right) \sqrt{T_s F_s} &= Q^{-1}(P_d^j) \sqrt{(1 + 2\gamma)} \\ Q^{-1}(P_f^j) - \gamma \sqrt{T_s F_s} &= Q^{-1}(P_d^j) \sqrt{(1 + 2\gamma)} \\ \sqrt{T_s F_s} &= \frac{1}{\gamma} \left[Q^{-1}(P_f^j) - Q^{-1}(P_d^j) \sqrt{(1 + 2\gamma)} \right] \\ T_s &= \frac{1}{F_s \gamma^2} \left[Q^{-1}(P_f^j) - Q^{-1}(P_d^j) \sqrt{(1 + 2\gamma)} \right]^2 \end{aligned} \quad (20)$$

Defining the sensing time with the last equation in Eq. (20), i.e., $T_s^{\text{con}} = T_s$, we can meet the requirement on false alarm and detection probabilities.

Because all SUs in k clusters have the same fixed sensing time slot, T_s^{con} , the sensing performances, i.e., false alarm and detection probabilities, depend on the SNR of an SU. Therefore, sensing performance is not improved with a fixed sensing time slot. In addition, the reporting time slots for the SU and the CH are not utilized by the 4G CRN.

5. Proposed superallocation and cluster-based cooperative spectrum sensing in the 5G CRN

In the 4G CRN approach, sensing time slots, reporting time slots of SUs, and reporting time slots of CHs are strictly divided as shown in **Figure 3**. Due to this rigid structure in the 4G CRN approach, the reporting time slots of other SUs and CHs are not used for spectrum sensing. However, these reporting time slots can be used in sensing the spectrum by other SUs by scheduling sensing and reporting time slots effectively. To this end, a superallocation and cluster-based cooperative spectrum sensing in the 5G CRN is proposed by increasing the sensing time slot. In the proposed 5G CRN, each SU can obtain longer sensing time slot because the other SU reporting times and the CH reporting times are merged to the SU sensing time. Therefore, the sensing time slots for SUs in the proposed 5G CRN can be longer than those in the 4G CRN.

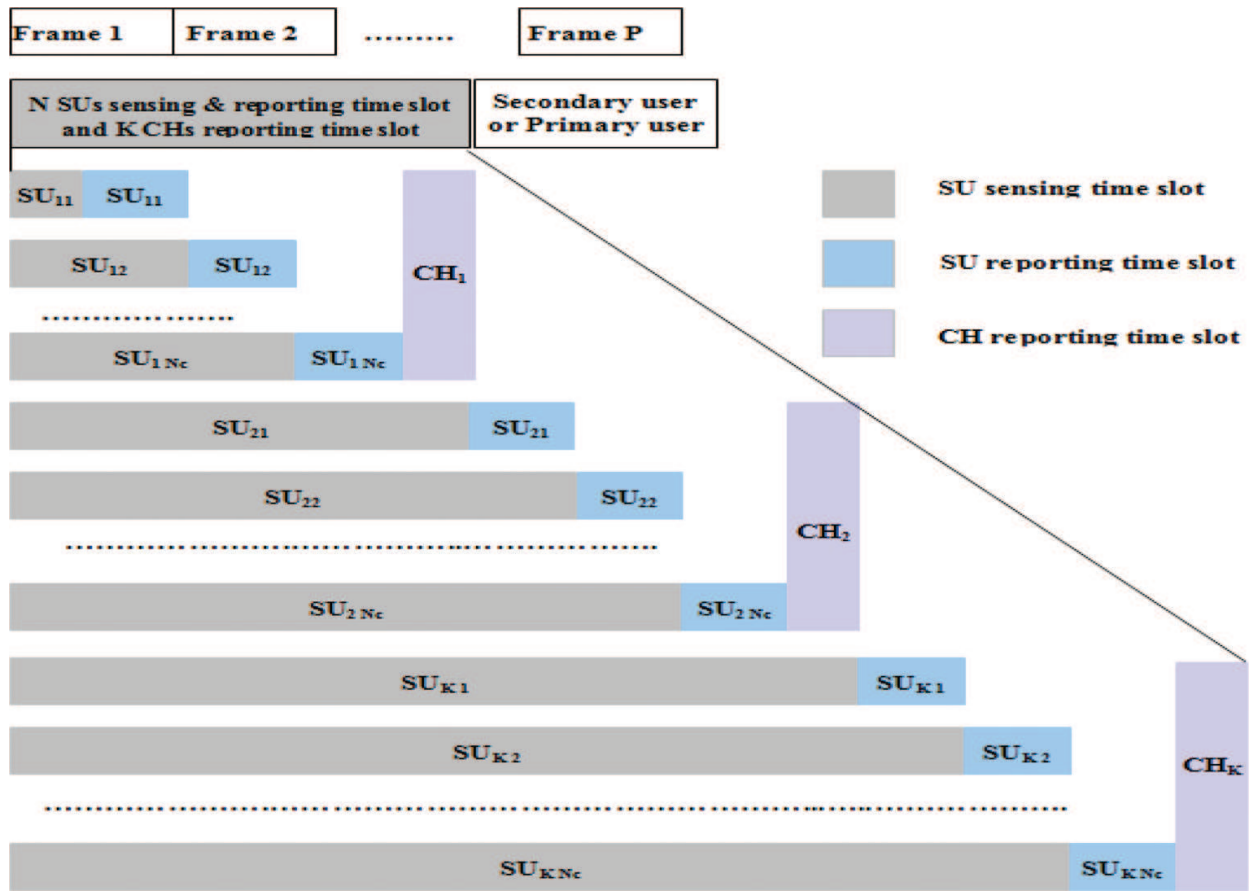


Figure 4. A superallocation and cluster-based cooperative spectrum sensing in the 5G CRN.

Figure 4 shows the proposed scheduling method of sensing and reporting time slots in the superallocation for cluster-based cooperative spectrum sensing in the 5G CRN. In the figure, SU_{nk} means the k th SU in the n th cluster in the network. To explain the duration of sensing time slot for SU_{nk} , we can define the durations of the sensing and reporting time for SU_{nk} with T_s^{nk} and T_r^{nk} , respectively.

In this proposed scheme, the sensing time slot for the first SU in the first cluster, i.e., SU_{11} , is equal to the sensing time slot in the 4G CRN, i.e., $T_s^{11} = T_s^{\text{con}} = T_s$. Except for SU_{11} , other SUs can obtain longer sensing time slots by scheduling SU reporting slots followed by the reporting slot for the CH of that cluster. With such a scheduling method, SUs can sense the spectrum during the reporting time slots of other SUs and CHs. For example, the sensing time slot of SU_{12} , T_s^{12} is equal to the total duration of sensing time slot and the reporting time slot of the SU_{11} , i.e., $T_s^{12} = T_s + T_r^{11}$. Similarly, T_s^{13} becomes the sum of the sensing duration of SU_{12} and the reporting duration of SU_{12} , i.e., $T_s^{13} = T_s^{12} + T_r^{12} = T_s + \sum_{i=1}^2 T_r^{1i}$. Obviously, the relationship of the sensing time slot $T_s^{1(j+1)}$ of the $SU_{1(j+1)}$ with the sensing time slot and the reporting time slot of the previous SUs can be given by

$$T_s^{1(j+1)} = T_s^{1j} + T_r^{1j} = T_s + \sum_{i=1}^j T_r^{1i} \quad (21)$$

for $j = 1, 2, 3, \dots, N_c$.

When $T_r^{\text{prop}} = T_r^{1j}$ for $j = 1, 2, 3, \dots, N_c$, the sensing time slot of the j th SU in the first cluster is written as

$$T_s^{1j} = T_s + (j-1)T_r^{\text{prop}} \quad (22)$$

Therefore, T_s^{1j} in the first cluster is greater than or equal to T_s^{con} .

For SU in the other clusters, the reporting time slots of SUs in the previous clusters and that of the previous CH can be used for a sensing time slot of SUs in the current cluster. Thus, T_s^{nj} is given by

$$\begin{aligned} T_s^{nj} &= \sum_{i=1}^{n-1} T_s^{iN_c} + \sum_{i=1}^k T_r^{ni} \\ &= (n-1)(T_s + N_c T_r^{\text{prop}} + T_{r,CH}^{\text{prop}}) + T_s + (j-1)T_r^{\text{prop}} \end{aligned} \quad (23)$$

Here, $T_{r,CH}^{\text{prop}}$ is the duration of the reporting time slot of a CH. Therefore, we can obtain longer sensing time as the index of CH increases.

5.1. Local sensing

As shown in Eq. (16), the detection probability P_d^j is a function of parameters λ_j , γ , and $T_s F_s$. For fixed F_s , γ and λ_j , P_d^j is a function of T_s , which can be represented as $P_d^j(T_s)$.

Lemma 3. In the proposed cluster-based cooperative spectrum sensing in the 5G CRN, the N SUs in the network adopts nonfixed sensing time slot $T_s^{nk} (\geq T_s^{\text{con}})$ in Eq. (23) to sense the PU's signal. Therefore, the sensing performance in the 5G CRN is improved over the 4G CRN.

Proof: Let $P_{d(\text{con})}^j$ and $P_{d(\text{prop})}^j$ denote the probability of detection for the conventional and proposed schemes, respectively. When SU belongs to the first cluster, the CH reporting time slot is not included in its sensing time. Here, the subscript "prop" means the proposed scheme in the 5G CRN.

Substituting the values of T_s and T_s^{1j} into Eq. (16), we have

$$P_{d(\text{con})}^j(T_s, \lambda_j) = Q\left(\left(\frac{\lambda_j}{\sigma_\eta^2} - \gamma - 1\right) \sqrt{\frac{T_s F_s}{(1 + 2\gamma)}}\right) \quad (24)$$

$$P_{d(\text{prop})}^{1j}(T_s^{1j}, \lambda_j) = Q\left(\left(\frac{\lambda_j}{\sigma_\eta^2} - \gamma - 1\right) \times \sqrt{\frac{(T_s + (j-1) \times T_r^{\text{prop}}) \times F_s}{(1 + 2\gamma)}}\right) \quad (25)$$

When the sensing time T_s^{1j} becomes longer, then obviously the detection probability $P_{d(\text{prop})}^j$ increases. Hence, we show that

$$P_{d(\text{prop})}^{1j} \geq P_{d(\text{con})}^j \quad (26)$$

Because $(T_s + (j-1) \times T_r^{\text{prop}}) \geq T_s^{\text{con}}$ for $j = 1, 2, 3, \dots, N_c$. When $j = 1$, then we obtain $P_{d(\text{prop})}^{1j} = P_{d(\text{con})}^j$.

If SU is not included in the first cluster, $P_{d(\text{prop})}^{nj}$ denotes the probability of detection for the proposed scheme. In this case, the sensing time slot includes the CH reporting time slots. Substituting the value of T_s^{nj} into Eq. (16), we obtain

$$P_{d(\text{prop})}^{nj}(T_s^{nj}, \lambda_j) = Q \left(\left(\frac{\lambda_j}{\sigma_\eta^2} - \gamma - 1 \right) \times \sqrt{\frac{((n-1)(T_s + N_c T_r^{\text{prop}} + T_{r,\text{CH}}^{\text{prop}}) + T_s + (k-1)T_r^{\text{prop}}) \times F_s}{(1 + 2\gamma)}} \right) \quad (27)$$

Therefore, $P_{d(\text{prop})}^{nj}(T_s^{nj}, \lambda_j) > P_{d(\text{con})}^{(n-1)N_c+j}(T_s, \lambda_j)$.

Each SU makes a local hard decision d_j^{hd} as follows.

$$d_{nj}^{hd} = \begin{cases} 1, & \text{if } P_{d(\text{prop})}^{nj} > P_{f(\text{prop})}^{nj} \\ 0, & \text{Otherwise} \end{cases} \quad (28)$$

5.2. Cluster decision

At the n th CH, all local decisions d_{nj}^{hd} received from the SUs will be combined to make a cluster decision $Q_{d,n}^{\text{prop}}$ as follows:

$$Q_{d,n}^{\text{prop}} = \begin{cases} 1, & \sum_{j=1}^{N_c} d_{nj}^{hd} > \xi \\ 0, & \text{Otherwise} \end{cases} \quad (29)$$

where ξ is the threshold for the cluster decision.

5.3. Global decision

At the FC, all cluster decisions ($Q_{d,n}^{\text{prop}}$) received will be combined to make a global decision (G) about the presence or the absence of the PU signal by using a τ -out-of- K rule as follows:

$$G = \begin{cases} 1, & \text{if } \sum_{n=1}^K Q_{d,n}^{\text{prop}} \geq \tau : H_1 \\ 0, & \text{Otherwise} : H_0 \end{cases} \quad (30)$$

where τ is the threshold for the global decision.

6. Simulation and result analysis

To evaluate the performance of the proposed cluster-based cooperative spectrum sensing in the 5G CRN, Monte Carlo simulations were carried out under following conditions:

The number of SUs is 12.

The number of clusters is 3.

The number of SUs in each cluster is 4.

The durations of sensing, SU reporting, and CH reporting time slots are 1 ms.

Average SNR of each SU in a cluster is -17 dB.

The PU signal is a BPSK signal.

The noise in SUs is CSCG.

The number of samples is 300.

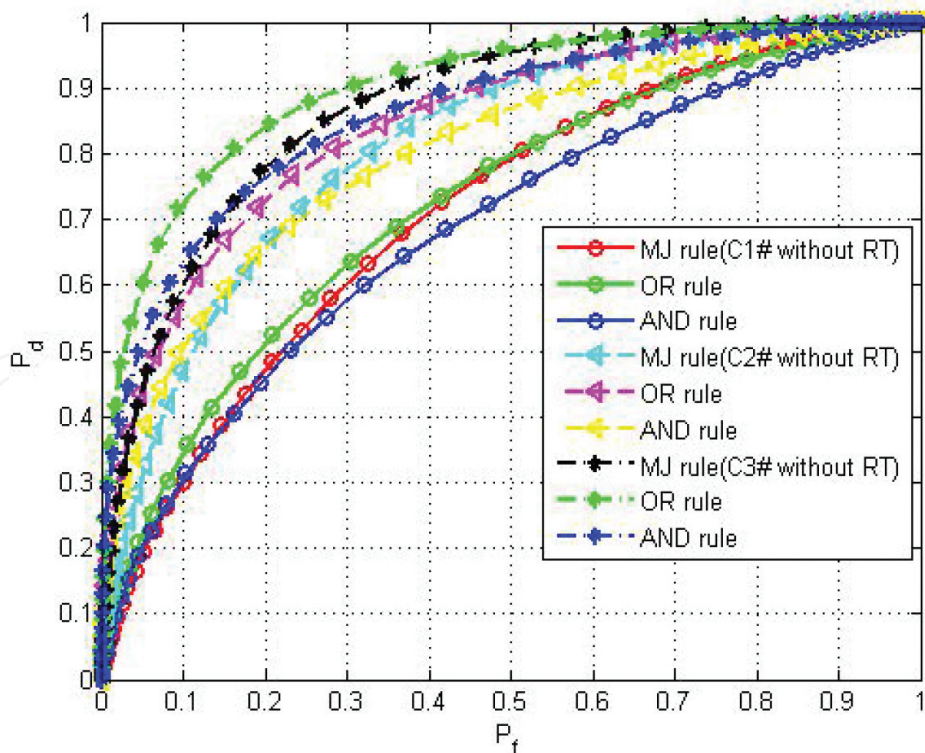


Figure 5. ROC curves of the proposed 5G scheme without cluster reporting time where C1#, C2#, and C3# mean the first, second, and third clusters, respectively.

First, the sensing performance of the proposed 5G and 4G cluster-based schemes, in terms of receiver operating characteristic (ROC), was evaluated under a CSCG channel. In this simulation, each SU conducts local sensing using equal gain combining (EGC).

Figures 5 and 6 show ROC curves for the proposed 5G cluster-based schemes without and with cluster reporting time (RT), respectively. The proposed 5G scheme outperforms in the detection of the PU compared with the 4G scheme because the proposed superallocation technique can have longer sensing time than the 4G one. Test statistics (Eq. (25)) was considered for the proposed 5G scheme without reporting time for the cluster decision. In addition, test statistics (Eq. (27)) was considered for the proposed 5G scheme with reporting time for the cluster decision. When the index of the cluster increases from one to three, the detection probability increases (**Figures 7 and 8**).

From the detection efficiency of cooperative spectrum sensing, the probability of detection is 0.8 and the probability of false alarm is 0.2. However, in the worst environment, we need the probability of detection to be more than 0.9 and the probability of false alarm to be less than 0.1. In the 4G scheme, we can achieve these sensing performances with a longer sensing time slot but the throughput of the 4G cognitive radio network decreases. In the proposed 5G CRN, we can easily achieve more than 0.9 and less than 0.1 for the probabilities of detection and false alarm, respectively, because SU reporting time and CH reporting time merge to sense the PU signal without decreasing system throughput.

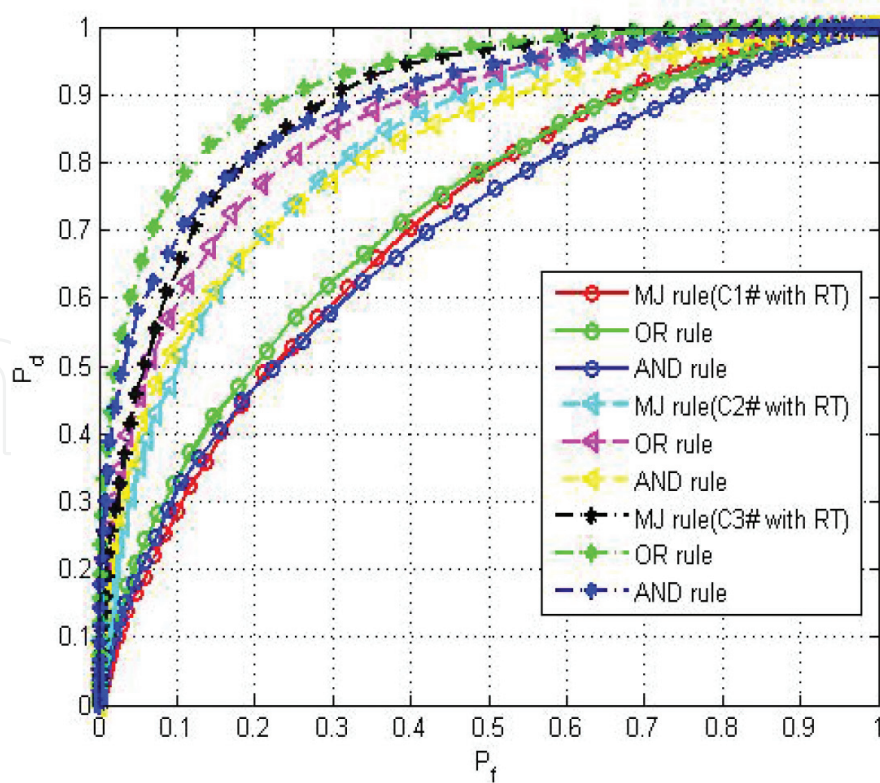


Figure 6. ROC curves of the proposed 5G scheme with cluster reporting time.

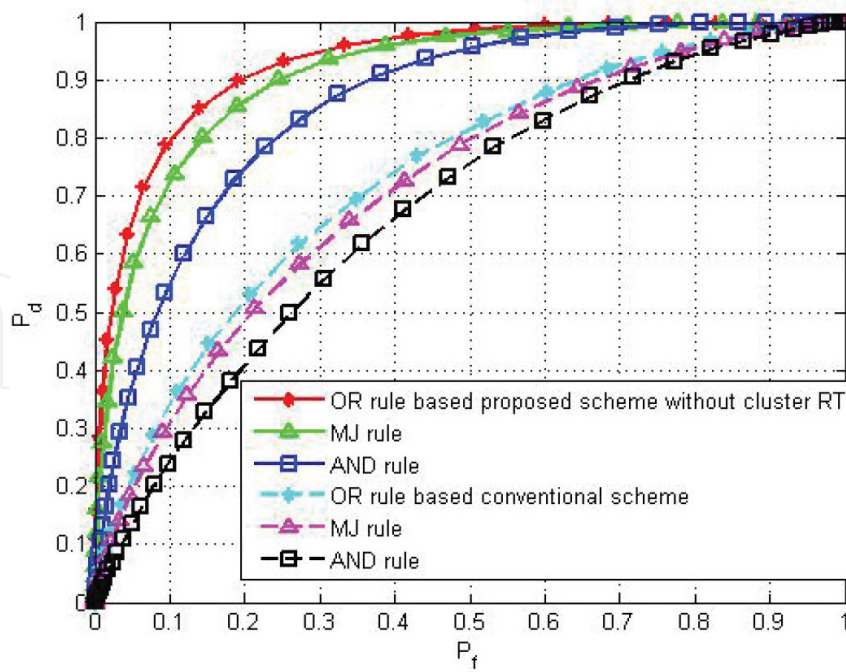


Figure 7. ROC curves of the proposed 5G scheme without cluster reporting time and the 4G scheme.

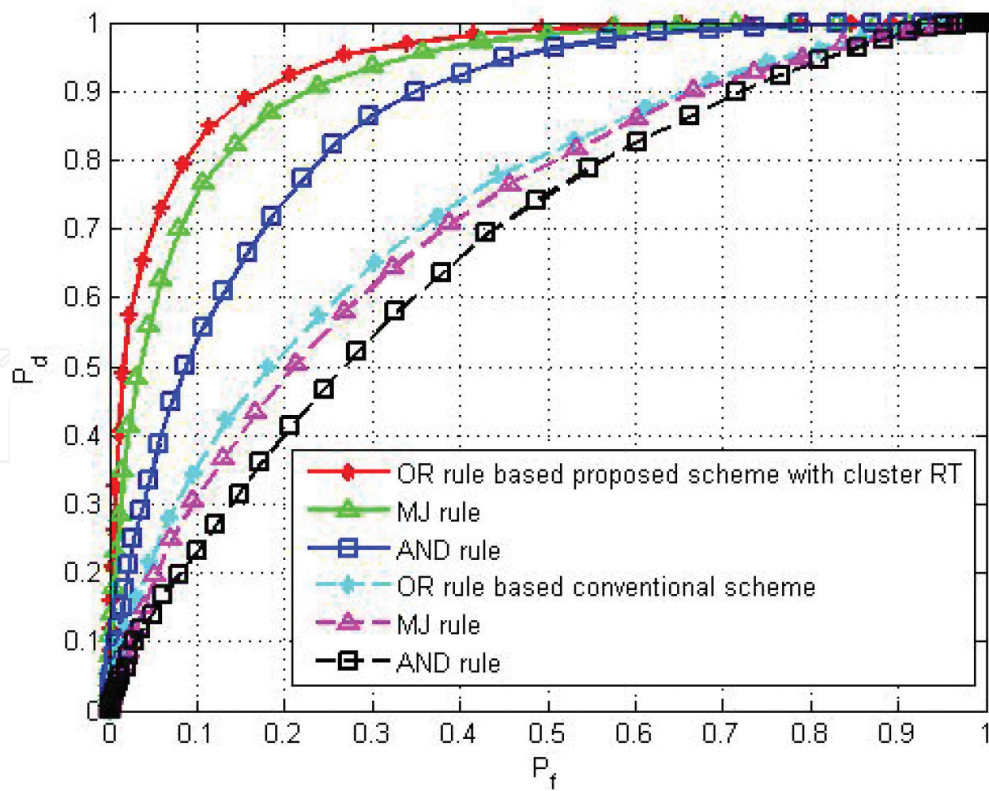


Figure 8. ROC curves of the proposed 5G scheme with cluster reporting time and the 4G scheme.

Second, the simulation was carried out under conditions whereby the SNRs of the PU's signal at the nodes are from -28 to -10 dB. The ROC curves of the proposed 5G scheme without

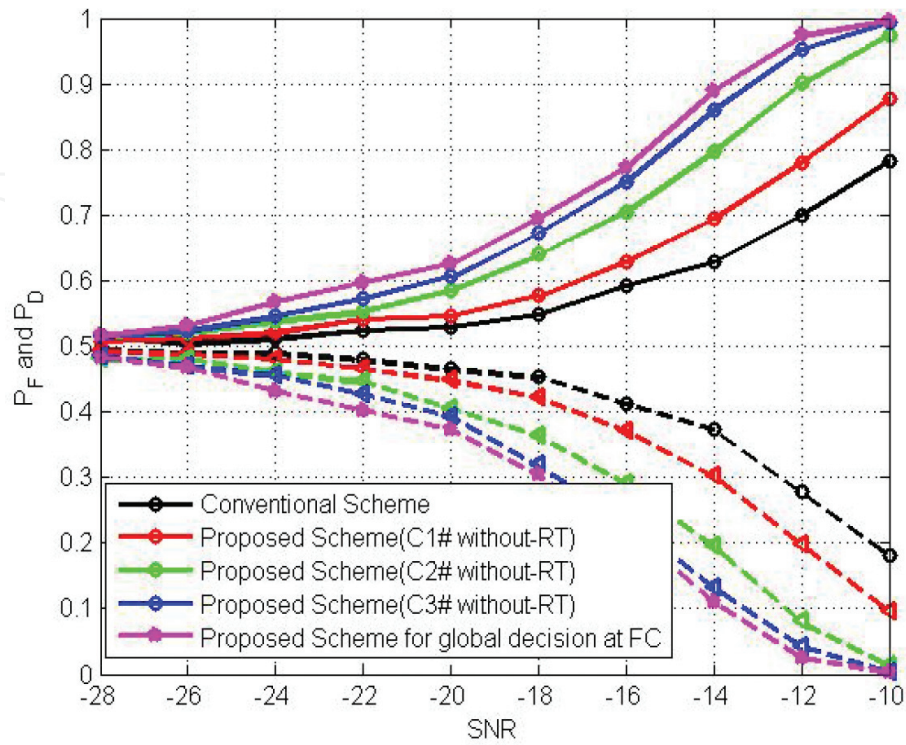


Figure 9. ROC curves of the proposed 5G scheme without cluster reporting time and the 4G scheme where SNRs of the PU's signal at the nodes are from -28 to -10 dB.

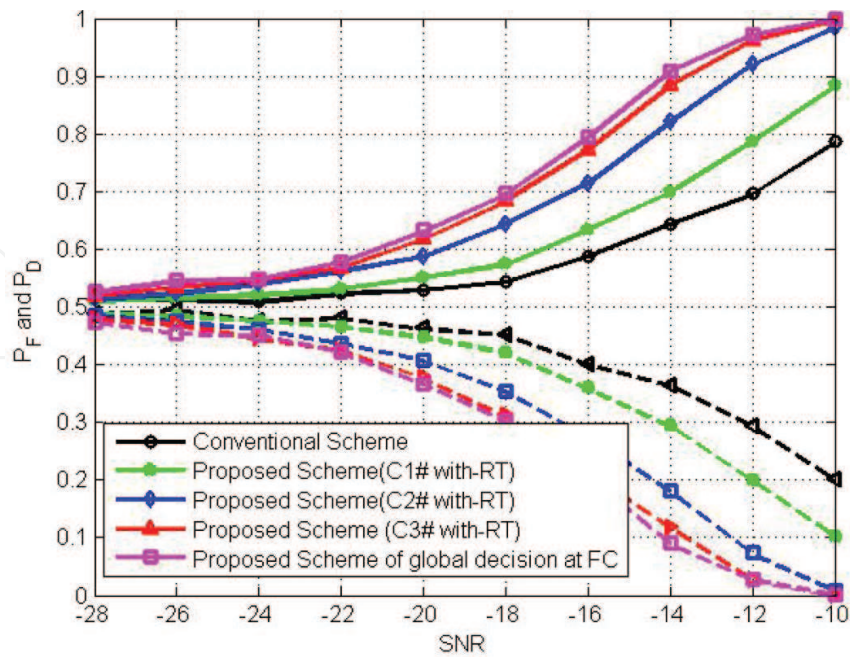


Figure 10. ROC curves of the proposed 5G scheme with cluster reporting time and the 4G scheme where SNRs of the PU's signal at the nodes are from -28 dB to -10 dB.

SNR		-28	-26	-24	-22	-20	-18	-16	-14	-12	-10
4G scheme		0.516	0.5042	0.5119	0.5248	0.5295	0.5487	0.5933	0.6286	0.6994	0.7825
Proposed 5G Scheme	Cluster 1	0.5073	0.5122	0.5209	0.5421	0.5473	0.5775	0.6290	0.6944	0.7810	0.8776
	Cluster 2	0.5154	0.5208	0.5378	0.5533	0.5860	0.6408	0.7055	0.7973	0.9006	0.9747
	Cluster 3	0.5149	0.5232	0.5453	0.5737	0.6061	0.6727	0.7507	0.8605	0.9528	0.9949
	Global	0.5160	0.5324	0.5682	0.5968	0.6264	0.6957	0.7733	0.8896	0.9734	0.9965

Table 1. Probability of detection (PD) without cluster reporting time under SNR versus number of clusters.

SNR		-28	-26	-24	-22	-20	-18	-16	-14	-12	-10
4G scheme		0.516	0.5042	0.5119	0.5248	0.5295	0.5487	0.5933	0.6286	0.6994	0.7825
Proposed 5G scheme	Cluster 1	0.5112	0.5170	0.5207	0.5316	0.5517	0.5743	0.6342	0.6993	0.7883	0.8835
	Cluster 2	0.5135	0.5236	0.5407	0.5628	0.5882	0.6445	0.7153	0.8217	0.9206	0.9844
	Cluster 3	0.5205	0.5346	0.5474	0.5684	0.6191	0.6845	0.7728	0.8849	0.9625	0.9972
	Global	0.5261	0.5460	0.5495	0.5790	0.6327	0.6963	0.7949	0.9093	0.9722	0.9995

Table 2. Probability of detection (PD) with cluster reporting time under SNR versus number of clusters.

cluster reporting time and the 4G CRN are illustrated in **Figure 9**. For our proposed 5G CRN scheme, it can be seen that the probability of detection increases as sensing time, T_s^{ij} , increases.

The ROC curves of the proposed 5G CRN scheme with cluster reporting time versus the 4G scheme are shown in **Figure 10**. **Figures 9** and **10** show that the probability of detection in the proposed 5G scheme with cluster reporting time is better than the proposed 5G scheme without cluster reporting time.

In **Tables 1** and **2**, the exact values of detection probabilities in the proposed 5G and 4G CRNs are shown. The gain of sensing performance can be verified with the results. For example, the proposed method with a cluster reporting time can detect the spectrum with nearly 100% detection probability whereas the 4G one detects the PU's signal with 78% of detection probability in -10 dB SNR.

7. Conclusion

In this chapter, we propose the superallocation and cluster-based cooperative spectrum sensing in a 5G CRN. The proposed 5G scheme can achieve better sensing performance in comparison with the cluster-based cooperative spectrum sensing 4G cognitive radio network. By rescheduling the reporting time slots of SUs and CHs, longer sensing durations are guaranteed for SUs depending on the order of reporting times of SU and CH. With simulations, the gain of performance is verified (**Tables 1** and **2**).

Author details

Md Sipon Miah^{1*}, Md Mahbubur Rahman¹ and Heejung Yu²

*Address all correspondence to: sipon@ice.iu.ac.bd

1 Department of Information and Communication Engineering, Islamic University, Kushtia, Bangladesh

2 Department of Information and Communication Engineering, Young Man University, Busan, South Korea

References

- [1] P. Demestichas, A. Georgakopoulos, D. Karvounas, K. Tsagkaris, V. Stavroulaki, J. Lu, C. Xiong, and J. Yao, "5G on the horizon: Key challenges for the radio-access network," *IEEE Vehicular Technology Magazine*, vol. 8, no. 3, pp. 47–53, Sep. 2013.
- [2] A. Zakrzewska, S. Rupp, and M. Berger, "Towards converged 5G mobile networks—challenges and current trends," in *Proceedings of the ITU Kaleidoscope Academic Conference*, St. Petersburg, Russian Federation, pp. 39–45, Jun. 2014.
- [3] J. Mitola and G. Q. Maguire, "Cognitive radio: Making software radios more personal," *IEEE Personal Communications*, vol. 6, no. 4, pp. 13–18, 1999.
- [4] B. Makki and T. Eriksson, "On the ergodic achievable rates of spectrum sharing networks with finite backlogged primary users and an interference indicator signal," *IEEE Transactions on Wireless Communications*, vol. 11, no. 9, pp. 3079–3089, 2012.
- [5] S. Haykin, "Cognitive radio: Brain-empowered wireless communications," *IEEE Journal of Selected Areas in Communications*, vol. 23, no. 2, pp. 201–220, 2005.
- [6] S. Enserink and D. Cochran, "A cyclostationary feature detector," in *Proceeding of Asilomar Conference on Signals, Systems and Computers*, vol. 2, pp. 806–810, 1994.
- [7] F. F. Digham, M. S. Alouini, and M. K. Simon, "On the energy detection of unknown signals over fading channels," *IEEE Transactions on Communications*, vol. 55, no. 1, pp. 21–24, 2007.
- [8] Y. Zeng and Y. C. Liang, "Maximum-minimum eigenvalue detection for cognitive radio," in *Proceeding of IEEE 18th International Symposium on Personal, Indoor and Mobile Radio Communications*, pp. 1–5, 2007.
- [9] I. F. Akyildiz, W. Y. Lee, M. C. Vuran, and S. Mohanty, "Next generation/dynamic spectrum access/cognitive radio wireless networks: A survey," *Computer Network*, vol. 50, no. 13, pp. 2127–2159, Sep. 2006.

- [10] D. Cabric, S. M. Mishra, and R W. Brodersen, "Implementation issues in spectrum sensing for cognitive radios," in *Proceeding of Conference Record of the Thirty-Eighty Asilomar Conference Signals, Systems and Computers*, vol. 1, pp. 772–776, 2004.
- [11] A. Ghasemi and E. S. Sousa, "Collaborative spectrum sensing for opportunistic access in fading environments," in *Proceeding of 1st IEEE International Symposium on New Frontiers in Dynamic Spectrum Access Networks*, pp. 131–136, 2005.
- [12] M. Mustonen, M. Matinmikko, and A. Mammela, "Cooperative spectrum sensing using quantized soft decision combining," in *Proceeding of 4th International Conference on Cognitive Radio Oriented Wireless Networks and Communications*, pp. 1–5, 2009.
- [13] S. Zarrin and T. J. Lim, "Composite hypothesis testing for cooperative spectrum sensing in cognitive radio," in *Proceeding of ICC'09 IEEE International Conference on Communications*, pp. 1–5, 2009.
- [14] J. F. Chamberland and V. V. Veeravalli, "The impact of fading on decentralized detection in power constrained wireless sensor networks," in *Proceeding of IEEE International Conference on ICASSP'4*, vol. 3, pp. 837–840, 2004.
- [15] T. C. Aysal, S. Kandeepan, and R. Piesiewicz, "Cooperative spectrum sensing over imperfect channels," in *Proceeding of IEEE GLOBECOM Workshops*, pp. 1–5, 2008.
- [16] T. C. Aysal, S. Kandeepan, and R. Piesiewicz, "Cooperative spectrum sensing with noisy hard decision transmissions," in *Proceeding of IEEE International Conference on Communications*, pp. 1–5, 2009.
- [17] C. Sun, W. Zhang, and K. Ben, "Cluster-based cooperative spectrum sensing in cognitive radio systems," in *Proceeding of IEEE International Conference on Communications, ICC'07*, pp. 2511–2515, Jun. 2007.
- [18] W. Xia, S. Wang, W. Liu, and W. Chen, "Cluster-based energy efficient cooperative spectrum sensing in cognitive radios," in *Proceeding of 5th IEEE International Conference on Wireless Communications, Networking and Mobile Computing, WiCom '09*, pp.1–4, 2009.
- [19] J. Jin, H. Xu, H. Li, and C. Ren, "Superposition-based cooperative spectrum sensing in cognitive radio networks," in *Proceeding of International Conference on Computer Application and System Modeling (ICCAASM)*, vol. 4, pp. 342–346, 2010.
- [20] W. B. Heinzelman, A. P. Chandrakasan, and H. Balakrishnan, "An application-specific protocol architecture for wireless micro sensor networks," vol. 1, no. 4, pp. 660–670, 2002.
- [21] T. Yucek and H. Arslan, "A survey of spectrum sensing algorithms for cognitive radio applications," in *Proceeding of IEEE Communications Surveys & Tutorials*, vol.11, no. 1, pp. 116–130, 2009.
- [22] H. Urkowitz, "Energy detection of unknown deterministic signals," in *Proceeding of IEEE*, vol. 55, no. 4, pp. 523–531, Apr. 1967.

- [23] V. I. Kostylev, "Characteristics of energy detection of quasideterministic radio signals," *Radiophysics and Quantum Electronics*, vol. 43, no. 10, pp. 833–839, Oct. 2000.
- [24] V. I. Kostylev, "Energy detection of a signal with random amplitude," in *Proc. of IEEE International Conference on Communications, ICC*, vol. 3, pp. 1606–1610, 2002.
- [25] K. X. Thuc and K. Insoo, "Cooperative spectrum sensing using Kalman filter based adaptive Fuzzy system for cognitive radio networks," *KSII Transactions on Internet and Information Systems*, vol. 6, no. 1, pp. 287–304, Jan. 2012.
- [26] S. Boyd and L. Vandenberghe, "Convex Optimization," Cambridge, UK: Cambridge University Press, 2003.
- [27] H. Mathis, "On the Kurtosis of digitally modulated signals with timing offsets," in *Proceeding of 3rd IEEE Signal Processing Workshop Signal Processing Advances Wireless Communications*, pp. 86–89, Mar. 2001.

